Fisheries and Oceans Canada | Pêches et Océans Canada
Ecosystems and Oceans Science | Sciences des écosystèmes et des océans

Canadian Science Advisory Secretariat (CSAS)

Research Document 2021/050

Central and Arctic Region

Abundance and total allowable landed catch estimates from the 2017 aerial survey of the Cumberland Sound beluga (*Delphinapterus leucas*) population

Cortney A. Watt[1]*, Marianne Marcoux[1]*, Mike Hammill[2], Leah Montsion[1], Claire Hornby[1], Bertrand Charry[3], J. Blair Dunn[1], Maha Ghazal[4], Roderick Hobbs[5], David S. Lee[6], Arnaud Mosnier[2], and Cory J.D. Matthews[1]

*First Authors

[1]Freshwater Institute
Fisheries and Oceans Canada
501 University Crescent
Winnipeg, MB, R3T 2N6

[2]Fisheries and Oceans Canada
850 route de la mer,
Mont-Joli, QC, G5H 3Z4

[3]Whale Seeker, Inc.
6243 rue Chambord
Montréal, QC, H2G3B8

[4]Government of Nunavut
Pangnirtung, NU, X0A 0R0

[5]Alaska Fisheries Center
National Marine Fisheries Service, NOAA
6130 NE 204th Street
Kenmore, WA, 98028

[6]Nunavut Tunngavik Incorporated
Department of Wildlife and Environment
Ottawa, ON, K1P 5E7

July 2021

Canada

Foreword

This series documents the scientific basis for the evaluation of aquatic resources and ecosystems in Canada. As such, it addresses the issues of the day in the time frames required and the documents it contains are not intended as definitive statements on the subjects addressed but rather as progress reports on ongoing investigations.

Published by:

Fisheries and Oceans Canada
Canadian Science Advisory Secretariat
200 Kent Street
Ottawa ON K1A 0E6

http://www.dfo-mpo.gc.ca/csas-sccs/
csas-sccs@dfo-mpo.gc.ca

ISSN 1919-5044
ISBN 978-0-660-39327-8 Cat. No. Fs70-5/2021-050E-PDF

Correct citation for this publication:

Watt, C.A., Marcoux, M., Hammill, M.O., Montsion, L., Hornby, C., Charry, B., Dunn, J.B., Ghazal, M., Hobbs, R., Lee, D.S., Mosnier, A., and Matthews, C.J.D. 2021. Abundance and total allowable landed catch estimates from the 2017 aerial survey of the Cumberland Sound beluga (*Delphinapterus leucas*) population. DFO Can. Sci. Advis. Sec. Res. Doc. 2021/050. iv + 33 p.

Aussi disponible en français :

*Watt, C.A., Marcoux, M., Hammill, M.O., Montsion, L., Hornby, C., Charry, B., Dunn, J.B., Ghazal, M., Hobbs, R., Lee, D.S., Mosnier, A., and Matthews, C.J.D. 2021. Estimations de l'abondance et du total autorisé des captures débarquées, d'après le relevé aérien de 2017 de la population de béluga (*Delphinapterus leucas*) de la baie Cumberland. Secr. can. de consult. sci. du MPO. Doc. de rech. 2021/050. iv + 35 p.*

TABLE OF CONTENTS

ABSTRACT

Cumberland Sound (CS) beluga (*Delphinapterus leucas*) are genetically differentiated and spatially segregated from other beluga populations, remaining in CS year-round. Under the Species at Risk Act the population is listed as Threatened. A survey in 2014 estimated approximately 1,150 (CV = 0.216) belugas in this population. A new series of visual and photographic surveys were flown during July and August 2017. The visual survey covered a larger area of CS than previous surveys, based on input from the Pangnirtung Hunters and Trappers Association, and was divided into three strata. The photographic survey provided full coverage of Clearwater Fiord, where CS beluga congregate in summer. Visual surveys of each of the three CS strata were flown twice, and analysed as a 600 m strip transect survey adjusted for perception and availability bias. The availability bias adjustment factor was calculated from whales equipped with satellite tags in 2006–2008 and was based on time spent in the upper 0–5 m for the visual survey (C_a = 2.54; CV = 0.050). Perception bias was calculated using duplicate sightings from the primary and secondary observers during the 2017 survey (C_p = 1.05; CV = 0.077). The photographic survey of Clearwater Fiord was conducted once during the first survey and four times during the second survey (using a weighted-CV average for the abundance estimate for the second survey) and adjusted to account for availability bias by evaluating the time spent in the 0–1 m or 0–2 m bin depending on beluga visibility (C_a = 4.46; CV = 0.117 and C_a = 2.06, CV = 0.056, respectively). The fully adjusted estimate for the two surveys of the entire area was 1,749 (CV = 0.423) and 1,379 (CV = 0.043) whales in Clearwater Fiord. This resulted in an average 2017 survey abundance estimate of 1,381 (CV = 0.043; 95% CI = 1,270–1,502) belugas, respectively. A model incorporating the 2017 and four previous survey estimates (1990–2014), along with harvest statistics from 1960–2017, was then fit using Bayesian inference to provide updated estimates of abundance and potential impacts of different harvest scenarios. The population model produced an estimated median abundance of 1,090 (CV = 0.207, 95% CI = 617–1,864) beluga in 2018. The model estimated 96% probability of stock decline in 10 years with the current annual quota (41) and a 0%, 25%, and 50% probability of population decline with harvests of 0, 14, and 20 beluga, respectively. PBR was calculated using reproductive rates of 0.04 (assumed for cetaceans) and 0.03 (estimated from the model) and varied from one to three animals, with a TALC of one to two whales.

INTRODUCTION

Current genetic and satellite telemetry evidence suggest beluga whales (*Dephinapterus leucas*) in Cumberland Sound (CS) form a distinct genetic population that remain within the sound year-round (de March et al. 2002, 2004, Richard and Stewart 2009, Turgeon et al. 2012). In the summer, large aggregations occur in Clearwater Fiord (Figure 1; Richard and Stewart 2009). Cumberland Sound belugas have been hunted commercially and for subsistence. Based on hunt records, abundance in 1923 was estimated at over 5,000 belugas (Mitchell and Reeves 1981). Commercial whaling, which ended in 1939, depleted the population to less than 1,000 individuals (Brodie et al. 1981, Richard 2013). The subsistence hunt has been regulated since the 1980s and the current quota is 41 beluga per year (Richard and Pike 1993). In 2017 the population was listed as Threatened under the Species at Risk Act (SARA).

DFO's current management objective is to increase the CS beluga population to 5,000 animals by 2091 (Marcoux and Hammill 2016). In 2016, a stochastic stock-production model, assuming density dependence acting on the population growth rate, was fitted by Markov Chain Monte Carlo (MCMC) Bayesian methods to aerial survey and reported harvest data (Marcoux and Hammill 2016). The model estimated the population at approximately 1,000 individuals and suggested that with the current quota of 41 animals the population would not increase to the interim target of 1,235 animals by 2026. The Pangnirtung Hunters and Trappers Association (HTA) raised concerns that low survey coverage in Kangilo Fiord and the southwestern portion of CS may have negatively biased the 2014 abundance estimate. To address these concerns, a survey with a modified design was flown in July and August 2017.

The goal of the present study was to estimate abundance of the CS beluga population based upon the 2017 survey and a population model that incorporates historical data to 1) provide advice to co-managers on the probability of population decline under different harvest scenarios and 2) calculate a new Total Allowable Landed Catch (TALC).

METHODS

STUDY AREA

The study area was divided into four strata, Kangilo Fiord, North CS, West CS, and Clearwater Fiord (Figure 1), and was designed to replicate the coverage of the 2014 aerial survey with modifications recommended by the Pangnirtung HTA. Based on recommendations from hunters, three new transects were added to the southern end of the West CS stratum. In addition, because most of the sightings during the 2014 visual survey occurred in Kangilo Fiord, this area was defined as its own stratum and the number of transect lines was increased (13 in 2017 compared to seven in 2014; Figure 1). The Kangilo Fiord, North CS, and West CS strata were surveyed visually. The Kangilo Fiord stratum comprised 13 transect lines spaced 2.5 km apart (Figure 1). The North CS stratum survey consisted of six parallel transects spaced 10 km apart, and the West CS stratum survey consisted of 18 parallel transects spaced 10 km apart. The Clearwater Fiord stratum consisted of 26 parallel transects spaced 700 m apart, resulting in complete coverage of the fiord. All transect lines were oriented perpendicular to the long-axis of each stratum. Two surveys were flown from July 29 to August 3 and from August 4 to 12.

VISUAL SURVEY

Surveys were flown in a DeHavilland Twin Otter (DH-6) equipped with four bubble windows and an optical glass covered camera hatch at the rear underbelly of the plane. Visual survey transects were flown at a target altitude of 1,000 ft (305 m) and a ground speed of 110 knots

(204 km/hr). A Global Positioning System unit (Bad Elf GPS pro+) was used to log the position, altitude, speed, and heading of the aircraft every second. Two synchronized iPads running Foreflight (a navigation application) were also connected to the Bluetooth GPS and used by the survey coordinator and pilots to input/edit waypoints for each transect, provide navigation and base maps, and record daily flight tracks. Surveys were only flown under the following environmental conditions: no rain, no risk of icing, ceilings of 2,500 ft or higher with no fog over the water in the survey area, and a Beaufort Sea State (BF) of 0–3 (although sea states of up to 4 were encountered during one survey [Table 1]). A double platform design in which two observers were seated at bubble windows on each side of the aircraft was used for all visual surveys (Buckland et al. 2001). All four observers remained in their respective positions in the plane throughout the survey. The two observers on the same side of the aircraft were visually and acoustically isolated from one another to ensure independent observations. The two primary observers at the front of the aircraft recorded the following environmental conditions at the start and end of each transect, and when any changes occurred: ice concentrations (in tenths), sea state (Beaufort scale), fog (% of field of view) and glare (% of forward field of view), and cloud cover (%). Beluga sightings were recorded on Sony PCM-D50 audio recorders; species, group size, and perpendicular declination angle to the center of each group, which was measured using a Peco DCC1 Digital Compass/Clinometer when the group was a beam of the observer, were recorded. A ‘group’ was defined as animals within one body length of each other and behaving cohesively. When time permitted, observers recorded additional details, such as the presence of calves, behaviour, and direction of travel. Photographs of the area below the aircraft were also taken during the visual surveys.

VISUAL SURVEY ANALYSIS

Visual line-transect survey data were analysed using Distance 6.2 software (Thomas et al. 2010), which requires the perpendicular distance of each observation from the trackline. This distance is calculated from the declination angle, which was measured for all but one of the observations. The perpendicular distance of that observation was estimated from an aerial photograph using (Equation 1):

$$D_S = \left[\left(\frac{(X_T - X_S)}{X_T} \text{ x } (2 \text{ x } \beta)\right)\right] \quad (1)$$

where D_S is the distance of the sighting, X_T is the total number of pixels in image widthwise, X_S widthwise pixel count from the image’s outer edge to the sighting, and β is half the field of view of the lens.

Buckland et al. (2001) suggest that at least 60–80 observations are required for reliable estimation of the detection function for line transect sampling; when there are a low number of detections only one or two additional sightings close to the trackline can affect estimation substantially. With only 26 total beluga sightings across all visual surveys, we decided to analyse the survey data using a strip-transect design. A hazard-rate function with a cosine adjustment was fitted to the sightings data and showed there was a relatively uniform distribution of sightings from 0–300 m, but animals were increasingly missed beyond this distance (Figure 2). Therefore, belugas observed within a 300 m (w) strip on either side of the aircraft were used to estimate near surface abundance.

Duplicate observations were removed and the probability density function of the perpendicular distances of beluga groups near the surface ($f(y)$) was estimated using a uniform function (Equation 2):

$$f(y) = \frac{1}{w} = 0.003 \quad (2)$$

The encounter rate ($E(n)$) was calculated using (Equation 3):

$$E(n) = \frac{n}{L} \qquad (3)$$

Where $n = \sum_{i=1}^{k} n_i$ is the total number of detections from line *i*, where *i* is 1 to *k* (total number of lines). The total survey effort (*L*) is $L = \sum_{i=1}^{k} l_i$, where *l* is transect length. The cluster encounter rate variance was calculated following Fewster et al. (2009) for systematic variance where (Equation 4):

$$var\left(\frac{n}{L}\right) = \frac{2k}{L^2(k-1)} \sum_{i=1}^{k-1} \left(\frac{n_i}{l_i} - \frac{n_{i+1}}{l_{i+1}}\right)^2 \qquad (4)$$

The density of belugas at or near the surface was estimated (Equation 5):

$$\widehat{D} = \frac{E(n) * f(0) * E(s)}{2 * L} \qquad (5)$$

The total number of belugas at or near the surface was estimated (Equation 6):

$$\widehat{N}_{sur} = \widehat{D} * A \qquad (6)$$

where *A* is the area of the survey stratum.

PERCEPTION AND AVAILABILITY BIASES

Conventional distance analysis assumes the probability of detection on the trackline (p(0)) is 1; however, observers may miss some whales that are visible on the trackline (Richard et al. 2010). Double observer methods, like those used in this study, allow for estimation of this 'perception bias'. To determine the value of p(0), duplicate sightings between the primary and secondary observers on each side of the aircraft were identified as occurring within 10 seconds and less than a 10 degree declination difference of one another (Pike and Doniol-Valcroze 2015).

Near surface abundance estimates were also adjusted to account for belugas that were diving and therefore unavailable to observers (i.e., availability bias) using the same values used to adjust the 2014 survey (Marcoux et al. 2016). In brief, availability bias was estimated by taking the weighted average of time spent in the 0–1 m bin, 0–2 m bin, 0–3 m bin, 0–4 m bin, and 0–6 m bin for three belugas tagged with satellite linked time depth recorder tags in Clearwater Fiord in July of 2006 (n = 1) and August 2007 (n = 2) (for tagging methodology see Orr et al. 2001). Weighted averages were based on the number of 6-hour blocks collected for each beluga. Standard errors were calculated using a weighted standard deviation divided by the square root of the number of belugas used in each calculation. Belugas can be seen to depths of 5 m when the water is clear (Richard et al. 1994), but tags were not programmed to collect information from 0–5 m, thus, an average of the availability bias for 0–4 m and 0–6 m was used to estimate the 0–5 m availability bias. The larger of the two standard errors was used as the standard error for the interpolated 0–5 m bin (Richard 2013). The availability bias adjustment factor, C_a, was calculated as (Equation 7):

$$C_a = \frac{1}{proportion\ spent\ in\ depth\ bin} \qquad (7)$$

For the visual survey, which was conducted over water we classified as clear (able to detect beluga up to 5 m below the surface of the water), we used an adjustment factor calculated using the interpolated 0–5 m bin.

The total estimate of belugas at or near the surface was adjusted to account for perception and availability biases using (Equation 8):

$$\widehat{N} = \widehat{N}_{sur} * C_p * C_a \quad (8)$$

The final abundance estimate had an associated variance calculated using the delta method (Buckland et al. 2001) where (Equation 9):

$$var(\widehat{N}) = \widehat{N}^2 \times \left\{ \frac{var(n/L)}{(n/L)^2} + \frac{var(\hat{E}(s))}{(\hat{E}(s))^2} + \frac{var(C_p)}{{C_p}^2} + \frac{var(C_a)}{{C_a}^2} \right\} \quad (9)$$

Confidence intervals were calculated assuming a log-normal distribution as suggested in Buckland et al. (2001).

PHOTOGRAPHIC SURVEY

The photographic surveys of the Clearwater Fiord stratum were flown 29 July, and 4, 7, 8, and 12 August at a target altitude of 2,000 ft (610 m) and speed of 110 knots (204 km/h). Complete photographic coverage of the stratum was achieved using two Nikon D810 cameras, equipped with 25 mm lenses, mounted at the rear of the aircraft and directed straight down, with the longest side perpendicular to the track-line. To georeference the photographs the cameras were linked via Bluetooth to a single GPS receiver (Bad Elf GPS Pro+) using a module accessory (Foolography Unleashed D200+ Bluetooth Module). Each camera was also connected to a laptop computer to control exposure settings, the photograph interval, and to save high resolution JPEG photographs to the computer's hard drive. At the target altitude of 2,000 ft, the ground area covered by each photograph was 875.4 m x 585.2 m, resulting in 20% overlap between photographs taken on adjacent transects. In theory, at the target speed and altitude, an interval of 9 seconds would result in 20% overlap between consecutive photographs along each transect. However, variations in speed, altitude, and pitch of the aircraft resulted in the need to use a shorter photographic interval of 7 or 8 seconds to achieve 20% overlap among photographs. Photographs were saved as JPEG files and downloaded at the end of each survey. When possible, surveys of Clearwater Fiord were flown to coincide with high tide, which provided better water clarity than low tide (Table 1).

PHOTOGRAPHIC SURVEY ANALYSIS

Photographs were examined for belugas by two experienced readers. The two analysts counted a common set of 673 photographs (21% of all photos) to assess inter-reader variation.

Photographs were georeferenced and examined in ArcMap 10.1 (ESRI). Issues with low visibility in some images due to under-exposure were resolved using Adobe Photoshop (Adobe Systems) by adjusting photograph brightness, contrast, levels, curves, exposure, vibrancy, saturation, and hue. Water clarity was evaluated in each photograph by looking at the proportion of the beluga body that could be seen in the photograph. An instantaneous availability bias adjustment factor for the 0–2 m bin was used for photographs where the reader could see the tail and/or the head of the belugas beneath the surface of the water and an adjustment for the 0–1 m bin was used if the photograph reader could only see the portion of the beluga body that was breaking the surface of the water. We compared the categorization of photographs requiring 0–1 m or 0–2 m corrections by the photograph readers to RGB pixel color of the water in each photograph. Pixels where water was brown was typically categorized as requiring an adjustment based on the 0–1 m bin, while blue pixels were typically identified as requiring the 0–2 m bin adjustment. This was done for each beluga that was identified and the number of beluga for which each category was applied for all repeats of Clearwater Fiord is shown in Table 2.

The surface area covered by each photograph was calculated as (Equation 10):

$$A_{photograph} = length * width \quad (10)$$

where length = altitude/F_s*L_s and width = altitude/F_s*W_s, and F_s is the focal length of the camera sensor (25 mm), L_s is the length of the camera sensor (35.9 mm) and W_s is the width of the camera sensor (24 mm).

For photographs with a proportion masked by sun glare, the reader created a shapefile to cover the glare and did not search for belugas within the glare area. The area covered by the glare was subtracted from the photograph area. The overlapping section between subsequent photographs was cropped from the first photograph. In addition, side overlap between adjacent line transects were cropped from the area of the adjacent line. Lastly, land area was cropped from the photographs by overlapping a shapefile of land with the photographs. The remaining area covered by water (with no glare) in each photograph was then calculated ($A_{noglare}$).

The number of belugas detected near or at the surface in each photograph was adjusted for the instantaneous availability bias, C_a described above, according to the clarity of the water.

An adjusted abundance estimate was calculated using (Equation 11):

$$\hat{N}_{cor} = C_a \times \hat{N}_{surface} \qquad (11)$$

where $\hat{N}_{surface}$ is the total number of belugas detected at the surface for each photograph.

Beluga density was calculated by dividing the summed beluga count by the summed area of glare-free water. Density was then multiplied by the stratum area to obtain near-surface abundance estimates (Equation12):

$$\hat{N}_{tot} = A_{stratum} \times \frac{\sum_{i=1}^{I} \hat{N}_{cor_i}}{\sum_{i=1}^{I} A_{noglare_i}} \qquad (12)$$

where $A_{stratum}$ is the area covered by the survey and I is the number of photographs per survey.

Within a single complete coverage photographic survey there is no variance associated with the encounter rate since all observable whales were counted. As a result, the only variance within a single repeat is the variance in the availability bias adjustment factor. However, four repeats of the Clearwater Fiord Stratum were conducted during the second visual survey (August 5–12) and therefore the abundance estimate was a weighted average (weighted by the CV) of the four repeats. The variance of this mean estimate was calculated using (equation 8.8, Buckland et al 2001) (Equation 13):

$$var(\hat{N}^*) = \frac{\sum_{i=1}^{4} A_i^2 var(\hat{N}_i)}{\left(\sum_{i=1}^{4} A_i\right)^2} \qquad (13)$$

where A_i is the area of the i^{th} repeat of the photographic survey.

The first survey of the Clearwater Fiord Stratum was applied to the first survey period with no variance associated with the estimate, only the variance from the availability bias adjustment factor.

COMBINED POPULATION ABUNDANCE ESTIMATE

The total population abundance was estimated by adding the individual stratum estimates for each survey period, with a variance calculated as the sum of the individual stratum variances.

MODEL SPECIFICATION

A stochastic stock-production model, assuming density dependence acting on the population growth rate was fitted by MCMC Bayesian methods to the aerial survey (1990–2017) and reported harvest data (1960–2018) (Table 3 and 4). We had two surveys in 2017 and used a weighted average (weighted by the CV) of the two surveys in the model. Observation error (associated with data collection and abundance estimation) was separated from the process error (arising from natural variability in population dynamics) using a hierarchical state-space model that considers survey data to be the outcome of two distinct stochastic processes: a state process and an observation process (de Valpine and Hastings 2002). The state process describes the underlying population dynamics and the evolution of the true stock size over time, using a discrete formulation of the Pella-Tomlinson model (Pella and Tomlinson 1969, Innes and Stewart 2002) was used by Marcoux and Hammill (2016) (Equation 14):

$$N_t = N_{t-1} + N_{t-1} * (\lambda_{max} - 1) * \left(1 - \left(\frac{N_{t-1}}{K}\right)^{\theta}\right) * \varepsilon_p - R_t \quad (14)$$

This version of the model multiplies the process error on the surplus production component of the equation and consequently only allowed positive growth in the absence of harvest. We used a slightly modified version of this model that allows the process error to have either positive or negative impacts on the growth rate as we believe this is more reflective of natural variation (Equation 15):

$$N_t = N_{t-1} * \left(1 + (\lambda_{max} - 1) * \left(1 - \left(\frac{N_{t-1}}{K}\right)^{\theta}\right)\right) * \varepsilon_p - R_t \quad (15)$$

Where: λ_{max} is the maximum growth rate or rate of population increase,

K is the environmental carrying capacity,

θ defines the shape of the density-dependent function,

ε_p is a stochastic term for the process error,

R_t are the removals for that year, calculated as reported catches, C_t, that are corrected for the proportion of animals that were struck and lost, $S\&L$ (Equation 16):

$$R_t = C_t * (1 + S\&L) \quad (16)$$

The observation process describes the relationship between true population size and observed data. In our model, aerial survey estimates S_t are linked to population size N_t by an error term, ε_{S_t} (Equation 17):

$$\ln(S_t) = \ln(N_t) + \varepsilon_{S_t} \quad (17)$$

The model was run 200,000 times with a 20,000 burn in and 30 thinning.

PRIORS

Priors were based upon Marcoux and Hammill (2016). Seven different trial models were used to evaluate the best population model for the CS beluga population (Table 5). Theta determines the shape of the density dependent function. For marine mammals, maximum productivity is thought to occur between 50% and 85% of carrying capacity (Taylor and DeMaster 1993), but different jurisdictions have used values of theta ranging between 1 and 3, which results in maximum productivity occurring between 50% and 63% (Wade 1998, Hobbs et al. 2015, Jackson et al. 2016, Heide-Jørgensen et al. 2016). Here we examined if theta was fixed and if it was allowed to vary between one and three (Table 5). For odontocetes, the maximum rate of population increase (λ_{max}) is thought to lie between 1.02 and 1.06, with most studies using 1.04 (Wade and Angliss 1997, Wade 1998, Lowry et al. 2008). In model 1, we fixed λ_{max} at 1.04, and in all other models we allowed the model to estimate λ_{max} using a uniform prior with minimum and maximum values ranging from 0.001–0.08 (Table 5). Reported harvests underestimate the number of belugas killed because some animals are wounded or killed but cannot be recovered (struck and lost [$S\&L$]). There are no data on $S\&L$ rates for CS, thus, we used the same $S\&L$ factor used by Marcoux and Hammill (2016) which also includes non-reporting (Table 6).

The stochastic process error terms ε_p were given a log-normal distribution with a zero location parameter. The precision parameter for this log-normal distribution was assigned a moderately informative prior following a Gamma (1.5, 0.0005) distribution. These parameters were chosen so that the resulting error would have a coefficient of variation of 1%, since beluga stock dynamics are not highly variable (Marcoux and Hammill 2016).

Survey variance was incorporated into the fitting process by guiding the formulation of the prior distribution of the survey error. The survey error term ε_{S_t} followed a log-normal distribution with a zero location parameter. Its precision parameter was given a moderately informative prior following a Gamma (2.5, 0.4) distribution. These parameters were chosen so that the resulting CV of the survey estimates would have quartiles Q_1 and Q_3 of 0.35 and 0.55, which were the same used by Marcoux and Hammill (2016).

PARAMETER ESTIMATION AND MODEL DIAGNOSTICS

Posterior estimates of all the parameters were obtained using a Gibbs sampler algorithm implemented in JAGS (Plummer 2003). R2jags and coda packages developed in the R programming language were used to examine the results (R Core Team 2013). With any Markov Chain Monte Carlo (MCMC) simulation, it is important to check convergence of the sampled values to their stationary distribution (Brooks et al. 2004, King et al. 2010). Initial runs of the code were made to investigate convergence and mixing (i.e., the extent and spread with which the parameter space was explored by the chain), and autocorrelation.

We tested for mixing of the chains using Geweke's test of similarity between different parts of each chain (Geweke 1996). The Brooks-Gelman-Rubin (BGR) diagnostic, which compares the width of 80% Credible Interval (CI) of pooled chains with the mean of widths of the 80% CI of individual chains was used for convergence between chains (Brooks and Gelman 1998). The relative contributions of the parameters to the model were examined by estimating the p_D value, which is the 'effective' number of parameters being fitted (Spiegelhalter et al. 2002).

MODEL PROJECTIONS AND MANAGEMENT OBJECTIVES

We used the population model to estimate the probability of the CS beluga population decreasing with different harvest scenarios (hunts of 0, 10, 20, 30, and 41).

We also calculated a Potential Biological Removal (PBR) following Wade (1998) and divided PBR by $S\&L$ (1.42 [Marcoux and Hammill 2016]) to calculate a revised Total Allowable Landed Catch (TALC) for different scenarios (Equation 18).

$$PBR = 0.5 * R_{Max} * N_{Min} * F_R \quad (18)$$

Where: $N_{Min} = N / \exp(z \sqrt{\ln(1+CV^2)})$

N = the model estimate for the population size in 2018 or the abundance estimates from the 2017 surveys.

z = 0.842 for the 20^{th} percentile of the log-normal distribution of the estimated population size (Wade 1998).

R_{Max} = maximum rate of increase for the stock. The default for cetaceans when the rate is unknown is 0.04. We also used the rate determined by the population model. It was then multiplied by 0.5 to simulate the effect of logistic density dependent growth.

F_R = recovery factor set to 0.1 for a threatened declining stock (as recommended by Hammill et al. 2017).

The TALC is (Equation 19):

$$TALC = PBR \ / \ loss\ rate \qquad (19)$$

RESULTS

PERCEPTION AND AVAILABILITY BIASES

Eleven sightings were identified as potential duplicates between observer 1 and 2, based on time and declination angle (Pike and Doniol-Valcroze 2015). Of the 11 potential duplicate sightings, five were confirmed as duplicates by investigating photographs that were taken throughout the visual survey; to determine if observers identified the same whale/group of whales or whether these were unique whales, 10 photographs before and after the sighting were evaluated. Six of the potential duplicates were seen outside of the frame of the photographs, but were within a 5 degree declination difference (Southwell et al. 2002) and were therefore considered to be duplicates.

Both the primary and secondary observers missed observations at the track-line [g(0)]. Based on all observations from 0–550 m, the observers had probabilities of detection (p(0)) equal to 0.78 ± 0.158. The estimated p(0) of the two observers combined was 0.95 ± 0.070, which resulted in a perception bias adjustment factor (C_p) of 1.05 (CV = 0.077).

An availability bias correction factor of 2.54 (CV = 0.052) interpolated from the 0–4 m and 0–6 m bin was used to adjust surface abundance estimates for the visual survey outside of Clearwater Fiord and were the same factors used to adjust the 2014 survey (Marcoux et al. 2016). An availability bias correction factor of 4.46 (CV = 0.117) for the 0–1 m bin was used for instances where only beluga breaking the surface could been seen, while a correction of 2.06 (CV 0.056) for the 0–2 m bin was used in instances where the whale's body could be observed at the surface and under the water.

VISUAL SURVEY

Two surveys of all three visual strata were conducted. The Kangilo Fiord, North CS, and West CS strata were flown on August 1–3, while a second survey of these strata occurred on August 4 and 5 (Figure 3). Due to weather constraints, the West CS stratum was only partially surveyed during the second survey (eight transect lines in the south could not be completed [Figure 3]). The estimated number of belugas at the surface outside of Clearwater Fiord is 543 (CV = 0.502) and 35 (CV = 0.508) for the first and second surveys, respectively (Table 7). Adjusting for perception and availability bias gives an estimate of 1,448 (CV = 0.510) and 203 (CV = 0.515) belugas outside of Clearwater Fiord for the first and second visual surveys (Table 7).

PHOTOGRAPHIC SURVEY OF CLEARWATER FIORD

Repeat counts of 673 photographs were highly correlated (simple linear regression; adj r^2 = 0.995, $F_{1,671}$ = 1.208e+05, $p < 0.0001$, Figure 4). Counts for the first and repeat counts were the same for 632 of the 673 photographs. Twenty-one photographs differed by three or fewer belugas and five photographs differed by 4 to 8 belugas, resulting in a mean absolute difference of 0.16 belugas per photograph. Individual beluga sightings in Clearwater Fiord are presented in

Figure 5. The abundance estimate for the first photographic survey is 301 (CV = 0.096) while the weighted average estimate from the four repeats during the second survey is 1,286 (CV = 0.029) (Table 2).

POPULATION ABUNDANCE ESTIMATE

The total abundance estimate adjusted for perception and availability bias summed for the four strata is 1,749 (CV = 0.423; 95 % CI = 790–3,871) and 1,379 (CV = 0.043; 95% CI = 1,267–1,500) for the first and second surveys respectively (Table 8). The weighted average (weighted by the CV) for the two surveys is 1,381 (CV = 0.043; 95 % CI = 1,270–1,502).

MODEL RESULTS AND PROJECTIONS

Seven different models were assessed to evaluate the sensitivity of the model to different prior parameters (Table 5). All models showed a population that has declined since 1960, with a current population of approximately 1,200 animals (Figure 6). Six of the models had starting populations of approximately 3,000 animals, while model 3 had a starting population of approximately 7,000 animals. All models where theta was allowed to vary showed strong updating of the prior towards one. Model 3 also showed a strong updating of the rate of increase prior to values greater than 6%, which we consider unlikely. Models 6 and 7 were very similar. The lower limit of the carrying capacity prior appeared to be too high in model 6; thus, we selected model 7 as the best model.

Priors and posteriors for the selected model (Table 6) are shown in Figure 7. In this model, each chain for the variables carrying capacity (K), population size in 2018 (N_{2018}), process error, initial population size (N_{1960}), and $S\&L$ rate showed rapid convergence. The overall Gelman and Rubin's potential scale reduction factor for this model were all equal to one, indicating convergence of the chain (Gelman and Rubin 1992), and the Geweke's Convergence Diagnostic Z-scores are all between -1.96 and 1.96 (Geweke 1996).

The model shows the population has been declining since 1960 (Figure 8) and some updating of the starting (1960) population prior with an estimated median starting population of 2,884 and a carrying capacity (K) of 7,875 (Table 9). There was no updating of the prior for λ_{max} with a median of 1.03. The current median population abundance (N_{2018}) is 1,090 animals (Table 9).

The model predicts there is a 0%, 25%, and 50% probability of stock decline within 10 years with landed catches of 0, 14, or 20 beluga per year, respectively (Figure 9). The probability of a decline with the current quota (41) is 96%.

Using the 2017 survey abundance or the model population estimate for 2018, the calculated PBR, using a recovery factor of 0.1 (Hammill et al. 2017) and R_{Max} values of 0.04 (assumed) or 0.03 (predicted from the model), varied from one to three animals, while the TALC is one to two whales (Table 10).

DISCUSSION

The 2017 survey estimate of 1,381 (CV = 0.043; 95 % CI = 1,270–1,502) beluga in CS extended the time series of abundance estimates for this population and allowed us to update the population dynamics model, and use the model to estimate future abundance under different harvest scenarios. This survey estimate had the lowest confidence interval of any survey of CS beluga, primarily because many of the beluga were captured in the photographic survey of Clearwater Fiord; a full coverage survey which results in a small CV. In addition, a weighted average (weighted by the CV) was used for the four repeats in Clearwater Fiord, which further reduced the CV.

There are limitations with surveys that need to be considered. For instance, surveying during high tide when water clarity conditions were judged to have been better may have positively biased estuary counts, since belugas have been shown to move into estuaries during high tide and we did not survey adjacent strata at the same time (Ezer et al. 2008, Castellote et al. 2013, Simard et al. 2014). Similarly, general movements between strata could also bias estimates since survey estimates on different days within a season can change significantly (Gosselin et al. 2017). For instance, some whales may have moved out of Clearwater Fiord during survey days, but we cannot determine this since adjacent strata were not surveyed at the same time. In the future in would be beneficial to survey adjacent strata during each Clearwater Fiord photographic survey. In the 2017 survey, movement of whales may have occurred during the first survey (July 29) when much lower number of belugas were seen in the estuary and this was coupled with higher estimates of belugas in the Cumberland Sound strata; suggesting belugas were still moving into Cumberland Sound, and more specifically, Clearwater Fiord (corroborating comments by local HTA members to CJDM during the first week of the survey). However, arrays of passive acoustic monitors in Clearwater Fiord through the summer occupancy period during previous years indicate that beluga whales enter the Fiord (frequent calls detected) and then remain within the Clearwater Fiord stratum once they enter (no calls detected until migration out in September) (Booy 2018). Little movement into or out of the Clearwater Fiord stratum after the first survey week is supported by similar numbers of belugas in the stratum over the period the four replicate surveys were conducted (August 4–12).

Unfortunately, due to weather and time constraints the West stratum was not fully completed during the second survey; during the first survey of this stratum there was one beluga sighting on the final most southern transect line, but during the second partial survey of this stratum, no whales were seen on the final transect line. We cannot rule out the possibility that we have not covered the entire distribution of this beluga population, which may underestimate abundance. However, we do not believe we would have missed many whales since there is a general movement of whales into Clearwater Fiord and typically whale sightings outside of the fiord represent a small proportion of the population (see Table 3). Future surveys could extend the southern limit of this stratum, as suggested by the Pangnirtung Hunters and Trappers Association. Temporal and spatial considerations are particularly important for surveying this migrating beluga population, as the first survey may have still captured some migratory movements, where a high proportion of whales were seen outside of Clearwater Fiord, while in the second survey, most whales had moved into Clearwater Fiord. Future surveys should carefully consider timing to ensure belugas in their summer residency period.

The availability bias correction factors used to adjust the survey estimates are the best values currently available for CS beluga; however, they are derived from a small number of whales tagged in 2006–2008. In the future, it would be ideal to have correction factors that overlap spatially and temporally with the survey. This becomes especially important in Clearwater Fiord where large correction factors (4.46) are used to account for the silty nature of the fiord. In comparison, availability bias adjustments for Western Hudson Bay beluga in rivers relied on the time spent in the 0–2 m bin and resulted in a correction of 1.71 (Matthews et al. 2017), and in Cook Inlet, Alaska, where belugas are considered to be in very turbid water, the adjustment for availability bias using radio-transmitters was only 2.03 (Hobbs et al. 2000). This suggests we may be overestimating the availability bias, and new telemetry data are needed. We also use an average for all whales, but it is important to consider that communal behaviour of belugas in response to environmental conditions could make an average availability bias correction inappropriate for all survey days.

In visual surveys, the observers have a few seconds to detect whales at the surface and the use of an instantaneous availability bias may over-estimate abundance. Since it was not possible to correct for the time belugas were in view during the visual surveys given the small number of detections and the lack of detailed dive cycle data for CS belugas, we used an instantaneous availability bias correction for both the photographic and visual surveys. While appropriate for the photographic survey, time-depth recorder (TDR) dive data are necessary for calculating an adjustment factor that incorporates time in view for future visual surveys (e.g., Asselin and Richard 2011).

The estimated 2018 abundance from the population model was 1,090 animals. As in a previous assessment of CS beluga, we included harvest data in a density-dependent model fitted to the aerial survey estimates (Marcoux and Hammill 2016). The reported harvest data was incomplete, and we made an assumption that when harvest was not reported, the entire quota was taken. In addition, we assumed that catch is proportional to the population age structure (other than we assumed no calves were taken), but there may be sex/age biases in the harvest that we are unable to evaluate. The impact that this may have on the model results is unknown. Various model iterations were examined before narrowing in on parameters that reduced correlation between model parameters and also made biological sense with regards to what is known about CS beluga. In the previous assessment, we allowed theta to vary, and fixed the maximum rate of increase to 1.04. In this assessment, we fixed theta at 1, which has no impact on our results since the population is so much smaller than K and will remain so for several years (Marcoux and Hammill 2016). There are also some indications of high stress in this population (Trana 2014) and the maximum rate may be lower than values typically considered for odontocetes; therefore, we allowed the model to estimate the λ_{max}, and limited the upper range for the prior to 1.05 to reflect our concerns (Hobbs et al. 2015, Wade et al. 2012). We also believed that the 1960 starting population was much lower than carrying capacity and set upper limits on the priors taking into account earlier assessments. Based on hunt records, abundance in 1923 was estimated at over 5,000 belugas (Mitchell and Reeves 1981). Commercial whaling, which ended in 1939, depleted the population to less than 1,000 individuals (Brodie et al. 1981, Richard 2013). All models we evaluated indicated the population has declined since 1960 and predict a future population decline with a continued harvest of 41 whales.

One advantage of PBR is that it only requires a single survey abundance estimate to calculate the PBR level. However, variability in survey estimates results in PBR estimates that will fluctuate much more than would be expected given the dynamics of beluga populations. As a result, we used a population dynamics model to estimate current abundance, which considers the entire time series of survey estimates. The model was considered robust to the assumptions in its estimate of current abundance and therefore the modelled abundance was used to calculate the PBR rather than relying on the 2017 survey estimate.

For populations with unknown growth rates, the R_{Max} value for calculating PBR is typically set at an assumed rate (0.04) which may not be appropriate for all populations. In this study, the model estimated an R_{Max} of 0.03 for the CS beluga population which suggests that use of the default R_{Max} is incorrect, and will result in the population to decline (see Brandon et al. 2016). Although the recovery factor is supposed to compensate for this, it may not be sufficient (Hammill et al. unpublished data). The selected recovery factor also needs to be appropriate for the population under consideration as this has a large impact on the resulting PBR estimate. Hammill et al. (2017) advised that a factor of 0.1 be used for the CS beluga population. Based on the model results, using a PBR estimate from the 2017 survey estimate alone is likely to result in a decline in the CS beluga population. However, regardless of the R_{Max} value used in the PBR calculation, PBR estimates suggest that the sustainable harvest for this population is less than the current harvest.

For the reasons described above, we recommend using the population model and calculating a PBR from the model estimate of abundance and maximum rate of increase. This approach makes greater use of the available information with respect to beluga population dynamics, harvest data, and multiple abundance estimates and will tend to result in a more stable estimate of PBR (Marcoux and Hammill 2016). Regardless of whether PBR from the survey abundance, PBR from the modelled abundance, or sustainable harvest advice is generated from the model itself, it is evident that the CS beluga population will not increase under current harvest levels. In fact, the model predicts a TALC of 0, 14, or 20 beluga per year would result in a 0%, 25%, and 50% probability of decline in the CSB population in 10 years and a 96% probability of decline with the current quota of 41 whales per year.

ACKNOWLEDGEMENTS

Thanks to the Pangnirtung HTA for their recommendations and assistance with the survey. Also thanks to N. Mosesee who assisted with the survey, and pilots K. Kushneryk and S. Delgaty. We thank the late M. Kingsley for developing the initial population model, and T. Doniol-Valcroze and A. Mosnier for model improvements.

REFERENCES CITED

Asselin, N.C. and Richard, P.R. 2011. Results of narwhal (*Monodon monoceros*) aerial surveys in Admiralty Inlet, August 2010. DFO Can. Sci. Advis. Sec. Res. Doc. 2011/065. iv + 26 p.

Booy, K.V. 2018. Acoustic monitoring of beluga whales (*Delphinapterus leucas*): spatio-temporal habitat preference and geographic variation in Canadian populations. Thesis (M.Sc.) University of Manitoba, Winnipeg, MB. 108 p

Brandon, J.R., Punt, A., Moreno, P., and Reeves, R. 2016. Toward a tier system approach for calculating limits on human-caused mortality of marine mammals. ICES J. Mar. Sci. 74(3) 877–887. doi:10.1093/icesjms/fsw202

Brodie, P.F., Parsons, J.L., and Sergeant, D.E. 1981. Present status of the white whale (*Delphinapterus leucas*) in Cumberland Sound, Baffin Island. Rep. Int. Whal. Comm. 31: 579–582.

Brooks, S.P., and Gelman, A. 1998. Alternative methods for monitoring convergence of iterative simulations. J. Comp. Graph. Stats. 7: 434–455.

Brooks, S., King, R., and Morgan, B. 2004. A Bayesian approach to combining animal abundance and demographic data. Anim. Biodiversity Conserv. 27.1: 515–529.

Buckland, S.T., Anderson, D.R., Burnham, K.P., Laake, J.L., Borchers, D.L., and Thomas, L. 2001. Introduction to distance sampling: estimating abundance of biological populations. Oxford University Press, Oxford, U.K. 434 p.

Castellote, M., Leeney, R.H., O'Corry-Crowe, G., Lauhakangas, R., Kovacs, K.M., Lucey, W., Krasnova, V., Lydersen, C., Stafford, K.M., and Belikov, R. 2013. Monitoring white whales (*Delphinapterus leucas*) with echolocation loggers. Polar Biol. 36: 493–509. doi: 10.1007/s00300-012-1276-2

COSEWIC (Committee on the Status of Endangered Wildlife in Canada). 2004. COSEWIC assessment and update status report on the beluga whale *Delphinapterus leucas* in Canada. Committee on the Status of Endangered Wildlife in Canada. Ottawa, ON. ix + 70 p.

de March, B.G.E., Maiers, L.D., and Friesen, M.K. 2002. An overview of genetic relationships of Canadian and adjacent populations of belugas (*Delphinapterus leucas*) with emphasis on

Baffin Bay and Canadian eastern Arctic populations. NAMMCO Sci. Publ. 4: 17–38. doi:10.7557/3.2835.

de March, B.G.E., Stern, G., and Innes, S. 2004. The combined use of organochlorine contaminant profiles and molecular genetics for stock discrimination of white whales (*Delphinapterus leucas*) hunted in three communities on southeast Baffin Island. J. Cetacean Res. Manag. 6: 241–250.

de Valpine, P., and Hastings, A. 2002. Fitting Population Models Incorporating Process Noise and Observation Error. Ecol. Monogr. 72(1): 57–76. doi:10.2307/3100085.

Ezer, T., R., Hobbs, and Oey, L-Y. 2008. On the movement of beluga whales in Cook Inlet, Alaska: Simulations of tidal and environmental impacts using a hydrodynamic inundation model. Oceanogr. 21(4): 186–195.

Fewster, R.M., Buckland, S.T., Burnham, K.P., Borchers, D.L., Jupp, P.E., Laake, J.L., and Thomas, L. 2009. Estimating the encounter rate variance in distance sampling. Biometrics. 65(1): 225–236.

Gelman, A., and Rubin, D.B. 1992. Inference from iterative simulation using multiple sequences. Statist. Sci. 7(4): 457–511.

Geweke, J. 1996. Evaluating the accuracy of sampling-based approaches to the calculation of posterior moments. *In* Bayesian Statistics 4. Edited by J.M. Bernardo, J.O. Berger, A.P. Dawid, and A.F.M. Smith. Oxford University Press, Oxford, U.K. pp. 169–193.

Gosselin, J.-F., Hammill, M.O., and Mosnier, A. 2017. Indices of abundance of beluga (*Delphinapterus leucas*) in James Bay and eastern Hudson Bay in summer 2015. DFO Can. Sci. Advis. Sec. Res. Doc. 2017/067. iv + 25 p.

Hammill, M.O., Stenson, G.B., and Doniol-Valcroze, T. 2017. A management framework for Nunavik beluga. DFO Can. Sci. Advis. Sec. Res. Doc. 2017/060. v + 34 p.

Heide-Jørgensen, M.P., Hansen, R.G., Fossette, S., Nielsen, N.H., Borchers, D.L., Stern, H., and Witting, L. 2017. Rebuilding beluga stocks in West Greenland. Anim. Conserv. 20(3): 282–293.

Hobbs, R.C., Waite, J.M., an Rugh, D.J. 2000. Beluga, *Delphinapterus leucas*, group sizes in Cook Inlet, Alaska, based on observer counts and aerial video. Mar. Fish. Rev. 62(3): 46–59.

Hobbs, R.C., Wade, P.R., and Shelden, K.E.W. 2015. Viability of a small, geographically-isolated population of beluga whales, *Delphinapterus leucas*: effects of hunting, predation, and mortality events in Cook Inlet, Alaska. Mar. Fish. Rev. 77: 59-88.

Innes, S., and Stewart, R.E.A. 2002. Population size and yield of Baffin Bay beluga (*Delphinapterus leucas*) stocks. NAMMCO Sci. Publ. 4: 225–238. doi:10.7557/3.2846.

Jackson, J.A., Carroll, E.L., Smith, T.D., Zerbini, A.N., Patenaude, N.J., and Baker, C.S. 2016. An integrated approach to historical population assessment of the great whales: case of the New Zealand southern right whale. R. Soc. Open Sci. 3(3): 150669. doi: 10.1098/rsos.150669.

King, R., Gimenez, O., Morgan, B. and Brooks, S. 2010. Bayesian Analysis For Population Ecology. Chapman & Hall (CRC Press), USA. 442 p.

Lowry, L.F., Frost, K.J., Zerbini, A., DeMaster, D., and Reeves, R.R. 2008. Trend in aerial counts of beluga or white whales (*Delphinapterus leucas*) in Bristol Bay, Alaska, 1993–2005. J. Cetacean Res. Manage. 10(3): 201–207.

Marcoux, M., and Hammill, M.O. 2016. Model Estimate of Cumberland Sound beluga (*Delphinapterus leucas*) population size and total allowable removals. DFO Can. Sci. Advis. Sec. Res. Doc. 2016/077. iv +35 p.

Marcoux, M., Young, B.G., Asselin, N.C., Watt, C A., Dunn, J.B., and Ferguson, S.H. 2016. Estimate of Cumberland Sound beluga (*Delphinapterus leucas*) population size from the 2014 visual and photographic aerial survey. DFO Can. Sci. Advis. Sec. Res. Doc. 2016/037. iv + 19 p.

Matthews, C.J.D., Watt, C.A., Asselin, N.C., Dunn, J.B., Young, B.G., Montsion, L.M., Westdal, K.H., Hall, P.A., Orr, J.R., Ferguson, S.H., and Marcoux, M. 2017. Estimated abundance of the Western Hudson Bay beluga stock from the 2015 visual and photographic aerial survey. DFO Can. Sci. Advis. Sec. Res. Doc. 2017/061. v + 20 p.

Mitchell, E., and Reeves, R.R. 1981. Catch history and cumulative catch estimates of initial population size of cetaceans in the Eastern Canadian Arctic. Rep. Int. Whal. Comm. 31: 645–682.

Orr, J.R., Joe, R., and Evic, D. 2001. Capturing and Handling of White Whales (*Delphinapterus leucas*) in the Canadian Arctic for Instrumentation and Release. Arctic 54(3): 299–304.

Pella, J.J., and Tomlinson, P.K. 1969. A generalized stock production model. Inter-Am. Trop. Tuna Comm. 13(3): 420–496.

Pike, D., and Doniol-Valcroze, T. 2015. Identification of duplicate sightings from the 2013 double-platform High Arctic Cetacean Survey. DFO Can. Sci. Advis. Sec. Res. Doc. 2015/034. v + 22 p.

Plummer, M. 2003. JAGS: A program for analysis of Bayesian graphical models using Gibbs sampling. *In* Proceedings of the 3rd International Workshop on Distributed Statistical Computing. Edited by: K. Hornik, F. Leisch, and A. Zeileis. Vienna, Austria. pp. 1–8.

R Core Team. 2013. R: A language and environment for statistical computing. R Foundation for Statistical Computing. Vienna, Austria.

Richard, P.R. 2013. Size and trend of the Cumberland Sound beluga whale population, 1990 to 2009. DFO Can. Sci. Advis. Secr. Res. Doc. 2012/159. iii + 28 p.

Richard, P.R., and Pike, D.G. 1993. Small whale co-management in the Eastern Canadian Arctic: A case history and analysis. Arctic 46(2): 138–143.

Richard, P., and Stewart, D.B. 2009. Information relevant to the identification of critical habitat for Cumberland Sound belugas (*Delphinapterus leucas*). DFO Can. Sci. Advis. Secr. Res. Doc. 2008/085: iv + 24 p.

Richard, P., Weaver, P., Dueck, L., and Baber, D. 1994. Distribution and numbers of Canadian High Arctic narwhals (*Monodon monoceros*) in August 1984. Meddelelser Om Grønl. Biosci. 39: 41–50.

Richard, P.R., Laake, J.L., Hobbs, R.C., Heide-Jørgensen, M.P., Asselin, N., and Cleator, H. 2010. Baffin Bay narwhal population distribution and numbers: Aerial surveys in the Canadian high Arctic, 2002–04. Arctic. 63(1): 85–99.

Simard, Y., Loseto, L., Gautier, S., Roy, N. 2014. Monitoring beluga habitat use and underwater noise levels in the Mackenzie Estuary: Application of passive acoustics in summers 2011 and 2012. Can. Tech. Rep. Fish. Aquat. Sci. 3068: vi + 49 p.

Spiegelhalter, D.J., Best, N.G., Carlin, B.P., and van der Linde, A. 2002. Bayesian measures of model complexity and fit. J. Royal Statist. Soc. Ser. B Statist. Methodol. 64(4): 583–639. doi:10.1111/1467-9868.00353.

Southwell, C., de la Mare, W., Underwood, M., Quartararo, F. and Cope, K. 2002. An automated system to log and process distance sight-resight aerial survey data. Wildlife Soc. Bull. 30(2): 394–404.

Taylor, B.L., and DeMaster, D.P. 1993. Implications of non-linear density dependence. Mar. Mammal Sci. 9(4): 360–371. doi:10.1111/j.1748-7692.1993.tb00469.x.

Thomas, L., Buckland, S.T., Rexstad, E.A., Laake, J.L., Strindberg, S., Hedley, S.L., Bishop, J.R.B., Marques, T.A., and Burnham, K.P. 2010. Distance software: design and analysis of distance sampling surveys for estimating population size. J. Appl. Ecol. 47: 5–14. doi:10.1111/j.1365-2664.2009.01737.x.

Trana, M.R. 2014. Variation in blubber cortisol as a measure of stress in beluga whales of the Canadian Arctic. Thesis (M.Sc.) University of Manitoba, Winnipeg, MB. 74 p.

Turgeon, J., Duchesne, P., Colbeck, G., Postma, L., and Hammill, M. 2012. Spatiotemporal segregation among summer stocks of beluga (*Delphinapterus leucas*) despite nuclear gene flow: implication for the endangered belugas in eastern Hudson Bay (Canada). Conserv. Genet. 13(2): 419–433.

Wade, P.R. 1998. Calculating limits to the allowable human-caused mortality of cetaceans and pinnipeds. Mar. Mammal Sci. 14(1): 1–37.

Wade, P.R., and Angliss, R.P. 1997. Guidelines for assessing marine mammal stocks: report of the GAMMS workshop April 3-5, 1996, Seattle, Washington. U.S. Dep. Commer., NOAA Tech. Memo. NMFS-OPR-12: 93 p.

Wade, P.R., Reeves, R.R., and Mesnick, S.L. 2012. Social and behavioral factors in cetacean responses to overexploitation: are Odontocetes less resilient than Mysticetes? J. Mar. Biol. 2012: 1–15. doi: 10.1155/2012/567276.

TABLES AND FIGURES

Table 1. Summary of aerial survey work conducted in Cumberland Sound in August 2017.

Survey	Date	Time (EDT)	Stratum	Type	Survey Repeat	Transects	Time of high tide*	Beaufort sea state
1	29–Jul	15:47–18:50	Clearwater Fiord	Photograph	1	1–26	09:16 h 21:37 h	-
-	1–Aug	11:30–16:10	West	Visual	1	18–12	-	2–4
-	2–Aug	9:54–16:30	West	Visual	1	11–1	-	2
-	3–Aug	9:15–12:30	Kangilo Fiord	Visual	1	1–13	-	2
-	3–Aug	13:00–16:24	North	Visual	1	1–6	-	1
2	4–Aug	9:15–14:00	West	Visual	2	1–10	-	1
-	4–Aug	15:05–18:00	Clearwater Fiord	Photograph	2	1–26	03:04 h 15:24 h	1
-	5–Aug	9:33–12:00	Kangilo Fiord	Visual	2	1–13	-	1
-	5–Aug	12:45–15:15	North	Visual	2	1–6	-	1
-	7–Aug	13:45–17:10	Clearwater Fiord	Photograph	3	1–26	05:09 h 17:23 h	2
-	8–Aug	14:15–17:35	Clearwater Fiord	Photograph	4	1–26	05:44 h 17:58 h	0–1
-	12–Aug	09:35–13:00	Clearwater Fiord	Photograph	5	1–26	08:12 h 20:32 h	0–1

*Time of high tide from The Tides, Currents, and Water Levels Web Site (DFO).

Table 2. Abundance estimates from the photographic survey.

Survey	Date	Photographs (#)	Area (km^2)	Photographs with glare (#)	Area (km^2) without glare	$\hat{N}_{surface}$	$\hat{N}_{surface}$ accounting for glare	Beluga (#) 0–1 m availability bias applied	Beluga (#) 0–2m availability bias applied	$\hat{N}$	CV $\hat{N}$ (%)
1	29-Jul-17	583	117.64	0	117.64	83	84	54	29	301	9.58
2	4-Aug-17	726	127.47	59	122.93	503	522	0	503	1,046	5.58
2	7-Aug-17	655	124.14	0	124.14	741	741	5	736	1,538	5.62
2	8-Aug-17	581	119.56	58	119.05	630	633	77	553	1,489	6.33
2	12-Aug-17	668	126.17	148	124.61	503	509	132	371	1,370	5.74
AVERAGE	**-**	-	-	-	-	-	-	-	-	**1,286***	**2.94**$^{\alpha}$

*weighted by effort (sum of the areas of the photographs)

$^{\alpha}$ calculated based on the average variance weighted by effort (sum of the areas of the photographs)

Table 3. Previous and current estimates of Cumberland Sound beluga abundance within Clearwater Fiord, the area of main concentration, the estimated number of animals outside the fiord and the total. Surface estimates (Surf) are number of animals estimated at the surface, the factor to adjust the counts for animals not at the surface (Ca), estimates adjusted for animals below the surface (Corr), and coefficient of variation (CV). Complete photographic coverage occurred in Clearwater Fiord, while visual surveys occurred outside of Clearwater Fiord.

Year	**Clearwater Fiord**			**Outside Clearwater Fiord**			**Total**			**% outside**	**Survey method**	**Survey coverage**	**Reference**
	Surf	C_a	Corr	Surf	C_a	Corr	Surf	Corr	CV				
1990	459	2.57	1,180	0	2.54	0	459	1,180	0.10	0	complete photographic, visual systematic	Clearwater Fiord, North stratum	Richard 2013
1999	749	2.57	1,924	137	2.54	347	885	2,270	0.09	15	complete photographic, visual systematic	Clearwater Fiord, North and West strata	Richard 2013
2009	118	2.57	303	215	2.54	546	333	849	0.38	64	complete photographic, visual systematic	Clearwater Fiord, North and West strata	Richard 2013
2014	228	4.46 and 2.06	603	215	2.54	548	444	1,151	0.21	48	complete photographic, visual systematic	Clearwater Fiord, North and West strata	Marcoux et al. 2016
2017-1*	84	4.46 and 2.06	301	543	2.54	1,379	627	1,749	0.42	31	complete photographic, visual systematic	Clearwater Fiord, Kangilo Fiord, North and West strata	Present study
2017-2*	573	4.46 and 2.06	1,286	31	2.54	79	604	1,379	0.04	6	complete photographic, visual systematic	Clearwater Fiord, Kangilo Fiord, North and West strata	Present study

*An average (weighted by the CV) of the two surveys from 2017 was used as the 2017 abundance estimate in the model.

Table 4. Reported harvests and quotas of Cumberland Sound belugas 1960–2018. Data for 1960 to 1972 are from Stewart (2004 unpubl. rep.); 1973–1976 are from the Planning Committee for the Co-Management of Southeast Baffin Beluga (1994 unpubl. rep.), and 1977–2014 from DFO harvest statistics unpublished data. There was no reported harvest for several years since 2004. In those years, it was assumed that the entire quota was taken.

Year	Reported landed	Year	Reported landed	Quota
1960	155	1989	42	-
1961	60	1990	36	
1962	52	1991	31	35
1963	167	1992	35	35
1964	69	1993	15	35
1965	65	1994	35	35
1966	80	1995	31	35
1967	60	1996	41	35
1968	28	1997	47	35
1969	27	1998	35	35
1970	60	1999	50	35
1971	50	2000	37	35
1972	61	2001	39	35
1973	43	2002	41	41
1974	44	2003	46	41
1975	50	2004	-	41
1976	120	2005	-	41
1977	178	2006	52	41
1978	85	2007	48	41
1979	70	2008	-	41
1980	43	2009	-	41
1981	45	2010	-	41
1982	40	2011	42	41
1983	44	2012	-	41
1984	40	2013	-	41
1985	44	2014	-	41
1986	26	2015	18*	-
1987	40	2016	41	-
1988	46	2017	34	41

*significant ice in 2015 limited harvesting

Table 5. Trial runs of the population model which evaluated changes to theta, the carrying capacity, lambda$_{Max}$, and the start population. All model runs started with catch data from 1960, since catch data dating back to 1920 resulted in significant auto and serial correlation (see Marcoux and Hammill 2016). The function dgamma (8,0.0015) has 0.0275, 0.25,0.5, 0.75 and 0.975 quantiles at 3,466, 5,973, 7,687, 9,704, and 14,429 respectively.

Model	Theta	Carrying capacity (K)	Lambda$_{Max}$	Harvest start	Start Population
1	1	dgamma(8,0.0015)	1.04	1960	2,000–9,000
2	Uniform(1,3)	dgamma(8,0.0015)	Uniform(1.01–1.08)	1960	2,000–15,000
3	2	dgamma(8,0.0015)	Uniform(1.01–1.08)	1960	2,000–15,000
4	2.39	dgamma(8,0.0015)	Uniform(1.01–1.08)	1960	< K
5	Uniform(1,3)	dgamma(8,0.0015)	Uniform(1.01–1.08)	1960	< K
6	1	Uniform(5,000–30,000)	Uniform(1.001–1.08)	1960	2,000–5,000
7	1	Uniform(4,000–15,000)	Uniform(1.01–1.05)	1960	1,000–4,000

Table 6. Prior distributions, parameters and hyper-parameters used in the final population model. “dist.” denotes a hyper-parameter with its own prior distribution (from Marcoux and Hammill 2016).

Parameters	Notation	Prior distribution	Hyper-parameters	Values
Survey error (t)	ε_{st}	Log-normal	μ_s	0
			τ_s	*dist.*
Precision (survey)	τ_s	*Gamma*	α_s	*2.5*
			β_s	*0.4*
Process error (t)	ε_{pt}	Log-normal	μ_p	0
			τ_p	*dist.*
Precision (process)	τ_p	Gamma	α_p	1.5
			β_p	0.00005
Density dependence shape function	Θ	Fixed	-	1
			-	-
Struck-and-lost*	*S&L*	Beta	α_{sl}	3
			β_{sl}	4
Initial population	N_{1960}	Uniform	N_{upp}	4,000
			N_{low}	1,000
Carrying capacity	K	Uniform	K_{upp}	15,000
			K_{low}	2,000
$\text{Lambda}_{\text{Max}}$	λ_{max}	Uniform	-	1.01–1.05
			-	-

*struck and lost also includes non-reporting

Table 7. Survey coverage of each visual stratum. Encounter rate, CV of encounter rate (CV_{ER}), mean group size, and CV of group size (CV_{GS}) are provided for visual strata. Surface abundance and CV (CV_{SA}) and corrections for perception (C_p) and availability bias (C_a) are shown with their respective CVs, as well as fully adjusted abundance ($\widehat{N}$) and CV of abundance ($CV\widehat{N}$).

Survey #	Stratum	Area (km^2)*	Effort (km)	# Groups	Encounter Rate (groups/km)	CV_{ER} %	Mean Group Size	CV_{GS} %	$\widehat{N}_{surface}$	CV_{SA} %	C_p[γ]	CV_{Cp} %	C_a	CV_{Ca} %	$\widehat{N}$	CV $\widehat{N}$ %
1	NSCS	2,442	255	0	0	0	0	NA	0	-	-	-	-	-	-	-
1	KFCS	554	234	0	0	0	0	NA	0	-	-	-	-	-	-	-
1	WSCS	9,489	962	11	0.011	42.20	3	32.72	543	-	-	-	-	-	-	-
TOTAL	-	-	-	-	-	-	-	-	**543**	**50.21**	**1.05**	**7.31**	**2.54**	**5.18**	**1,448**	**51.00**
2	NSCS	2,442	255	0	0	0	0	NA	0	-	-	-	-	-	-	-
2	KFCS	554	234	1	0.004	99.40	1	NA[α]	4	-	-	-	-	-	-	-
2	WSCS	4,107	440	2	0.005	61.94	1	NA[β]	31	-	-	-	-	-	-	-
TOTAL	-	-	-	-	-	-	-	-	**35**	**50.76**	**1.05**	**7.31**	**2.54**	**5.18**	**203**	**51.47**

*Area of each stratum was calculated using a Lambert azimuthal equal-area (GRS80) projection in ArcGIS.

[α]A single whale was sighted in this stratum.

[β]Two groups of one whale sighted.

[γ]Combined perception bias calculated from all sightings from 0–550 m.

Table 8. Total CS beluga population abundance estimates from two surveys, 29 July–3 August and 4–12 August, 2017. The estimate for Clearwater Fiord for Survey 2 is a weighted average of four photographic surveys.

Survey #	Strata	Survey	Estimate	CV (%)	95% CI
1	North	Visual	0	-	-
1	Kangilo Fiord	Visual	0	-	-
1	West	Visual	1,448	51.00	-
1	Clearwater Fiord	Photographic	301	9.58	-
TOTAL	-	-	**1,749**	**42.27**	**790–3,871**
2	North	Visual	0		-
2	Kangilo Fiord	Visual	11	104.19	-
2	West	Visual	83	54.02	-
2	Clearwater Fiord	Photographic	1,286	2.94	**-**
TOTAL	-	-	**1,379**	**4.31**	**1,267–1,500**
AVERAGE*	-	-	**1,381**	**4.29**	**1,270–1,502**

*Weighted average (weighted by the CV) for the two surveys.

Table 9. Model outputs for the CS beluga stock model 7 (see Table 5). The mean, standard deviation (SD), median (50th Q), 25th and 75th quantiles (25th Q, 75th Q), 95% credibility intervals (2.5%CI, 97.5%CI) are given for the following model parameters and their priors: carrying capacity (K), maximum growth rate (λ_{max}) process error (process), survey precision (surv), starting population (startpop), struck and loss (S&L), and population size in 2018 (N_{2018}). $\hat{R}$ is the Brooks-Gelman-Rubin statistics; values near 1 indicate convergence of chains. N.eff is the number of effective chains after considering autocorrelation.

Parameter	Mean	SD	2.5%CI	25th Q	50th Q	75th Q	97.5%CI	$\hat{R}$	n.eff
K	8,233	3,567	2,907	5,067	7,875	11,258	14,607	1.001	5.00E+05
K.prior	8,489	3,752	2,321	5,238	8,486	11,730	14,678	1.001	470,000
$lambda_{Max}$	1.03	1.01	1.01	1.02	1.03	1.04	1.05	1.001	130,000
$lambda_{Max}$.prior	0.03	0.01	0.01	0.02	0.03	0.04	0.05	1.001	5.00E+05
error.process*	1.00	0,01	0.98	1.00	1,.00	1.00	1.02	1.001	413,103
prec.process	30,092	24,521	2,213	12,231	23,736	41,112	93,588	1.001	97,000
prec.process.prior	29,982	24,439	2,189	12,115	23,673	41,061	93,179	1.001	5.00E+05
prec.surv	6.97	3.30	2.09	4.56	6.45	8.82	14.79	1.001	5.00E+05
prec.surv.prior	6.25	3.95	1.04	3.34	5.44	8.28	16.06	1.001	370,000
startpop	3,077	537	2,042	2,667	3,100	3,519	3,946	1.001	160,000
startpop.prior	2,499	867	1,075	1,747	2,496	3,252	3,926	1.001	5.00E+05
S&L	0.38	0.16	0.10	0.25	0.36	0.49	0.72	1.001	3.00E+05
S&L.prior	0.43	0.18	0.12	0.30	0.42	0.55	0.78	1.001	5.00E+05
N_{2018}	1,127	320	617	915	1,090	1,293	1,864	1.001	450,000

*Mean value for the 59 years included in the model.

Table 10. Potential Biological Removal (PBR) and Total Allowable Landed Catch (TALC) estimates from the 2017 survey and from the model estimate (median) for 2018 using an assumed R_{Max} of 0.04 and the estimated R_{Max} from the model of 0.03, and using a recovery factor of 0.1 for a declining threatened population (Hammill et al. 2017).

R_{Max}	Method	N	CV	N_{min}	F_R	PBR	TALC
0.04	2017 Survey	1381	4.29	1332	0.1	3	2
-	Model	1090	20.74	917	0.1	2	1
0.03	2017 Survey	1381	4.29	1332	0.1	2	1
-	Model	1090	20.74	917	0.1	1	1

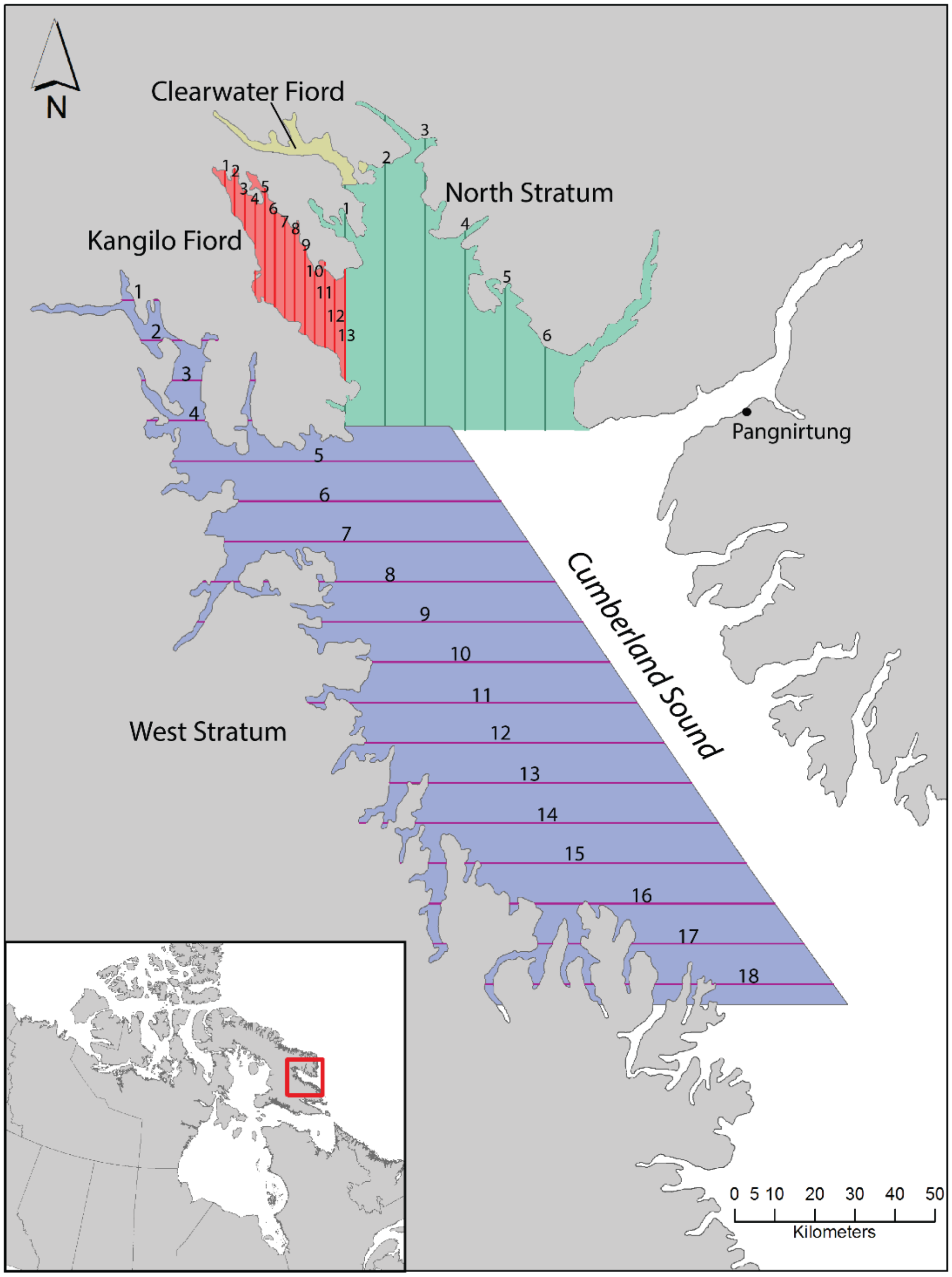

Figure 1. Map indicating three strata the transect lines surveyed in the visual aerial survey in Cumberland Sound in 2017.

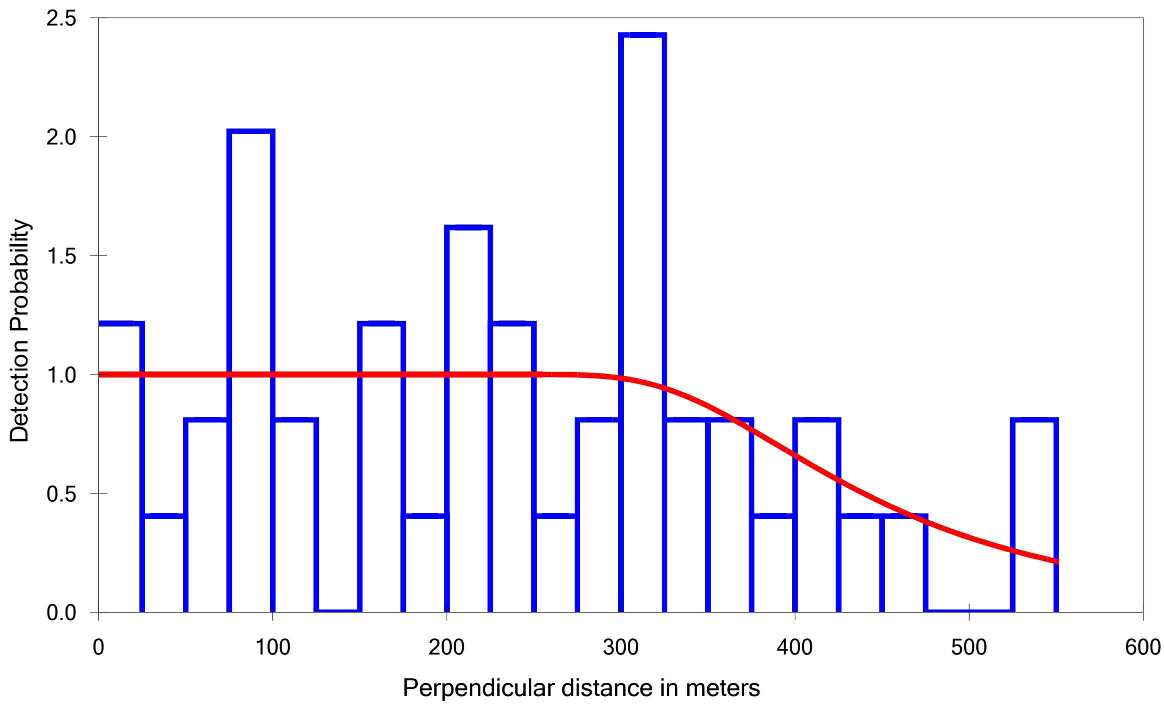

Figure 2. Histogram of the perpendicular distances of beluga sightings in the visual aerial survey in Cumberland Sound in August 2017.

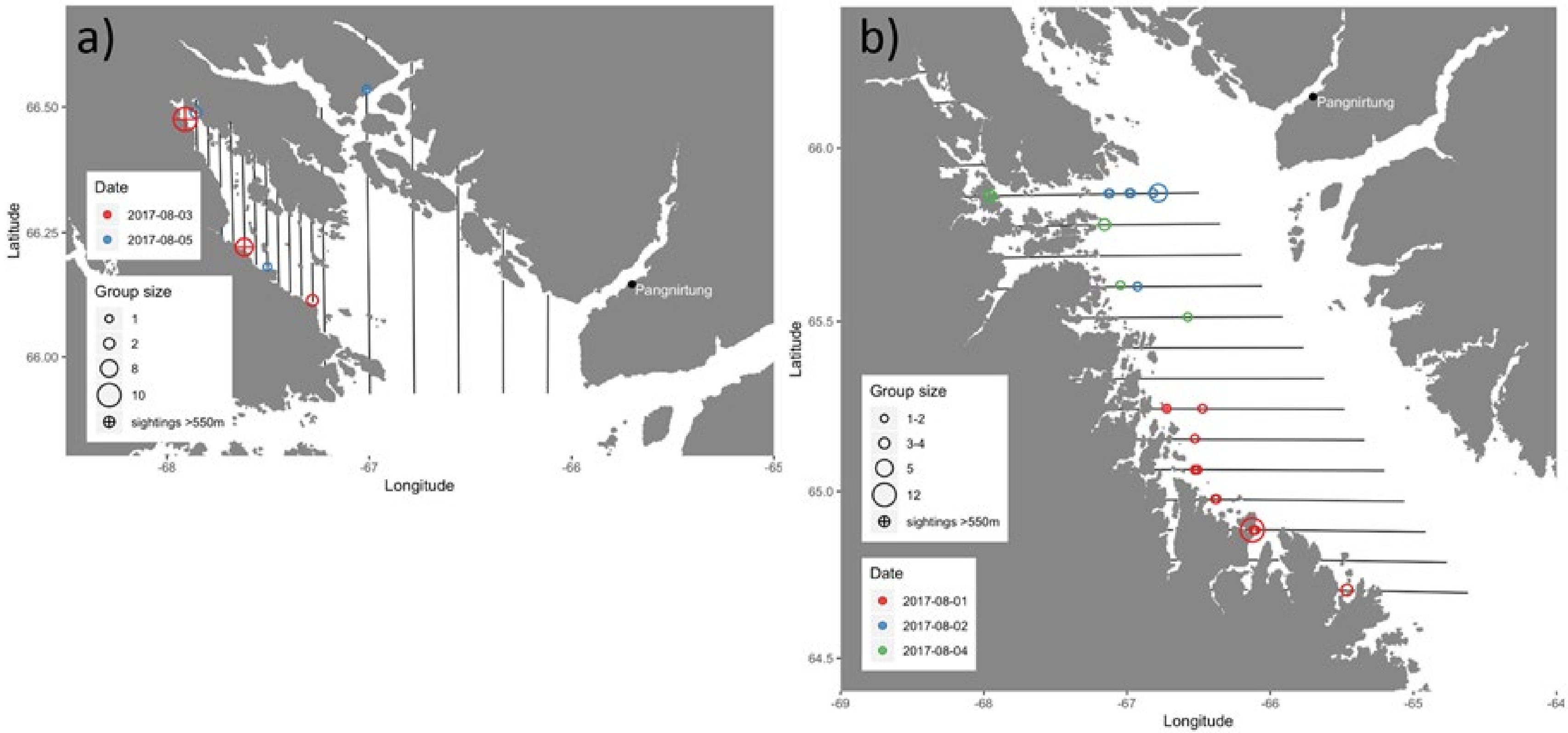

Figure 3. Maps of the transects for the a) Kangilo Fiord and North stratum and b) West stratum with beluga group size indicated. The West stratum was completely surveyed during survey 1, but due to weather constraints, was only partially surveyed during the second survey (the eight most southerly transect lines were not completed).

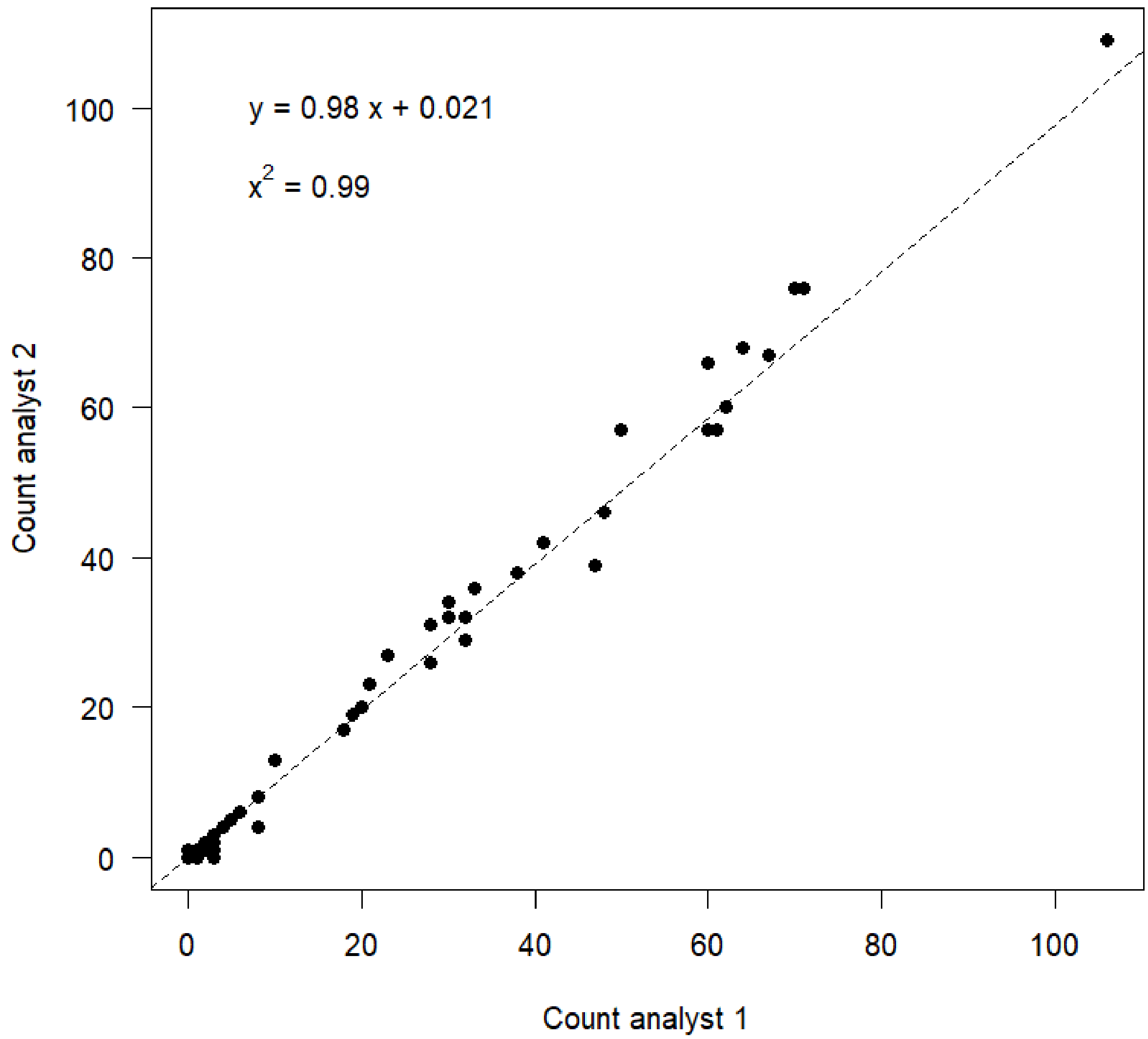

Figure 4. Comparison of photographic counts done by photograph analysts 1 and 2.

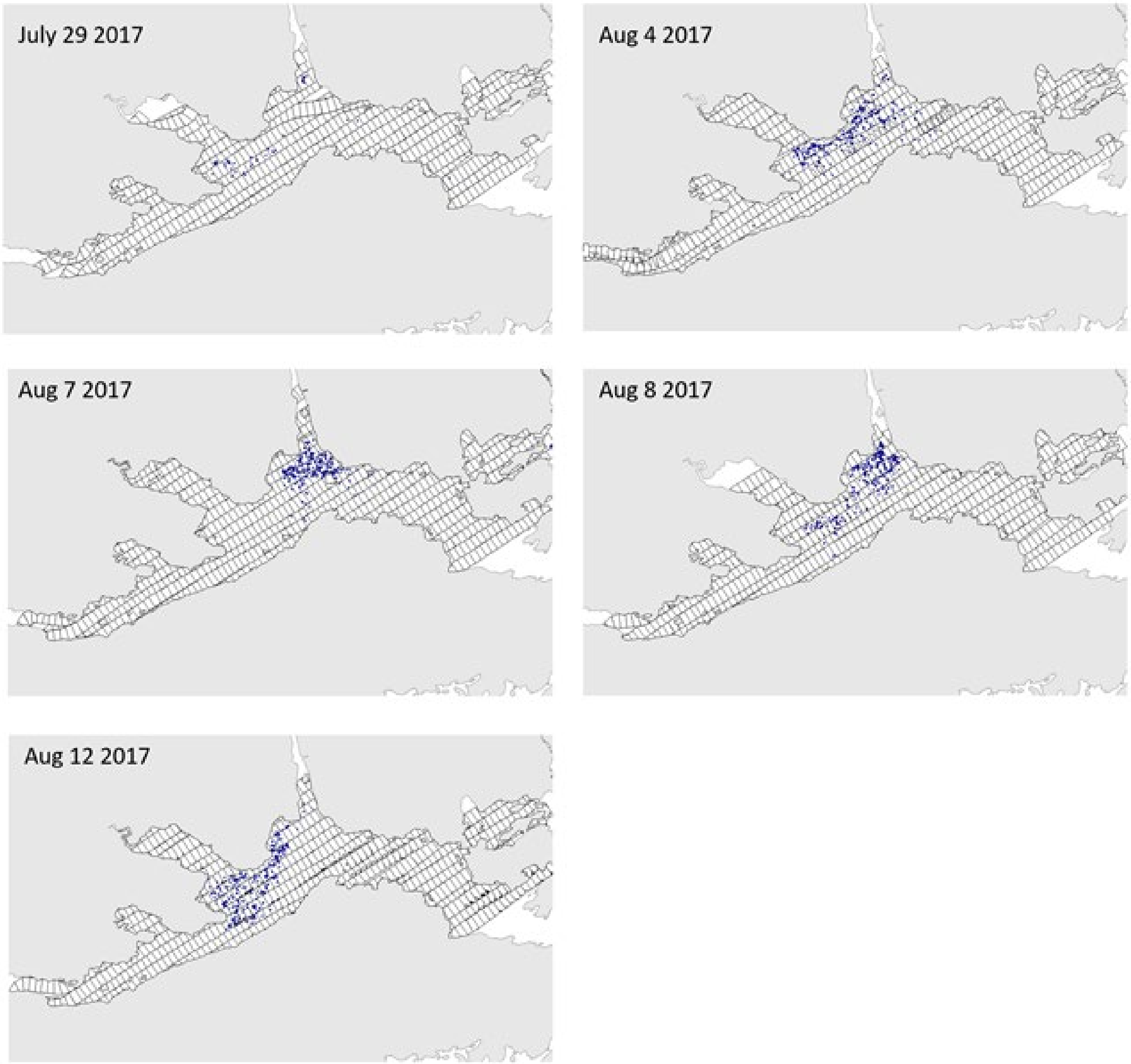

Figure 5. Map of the five photographic surveys of Clearwater Fiord showing individual beluga sightings and the geographic coverage of each photograph.

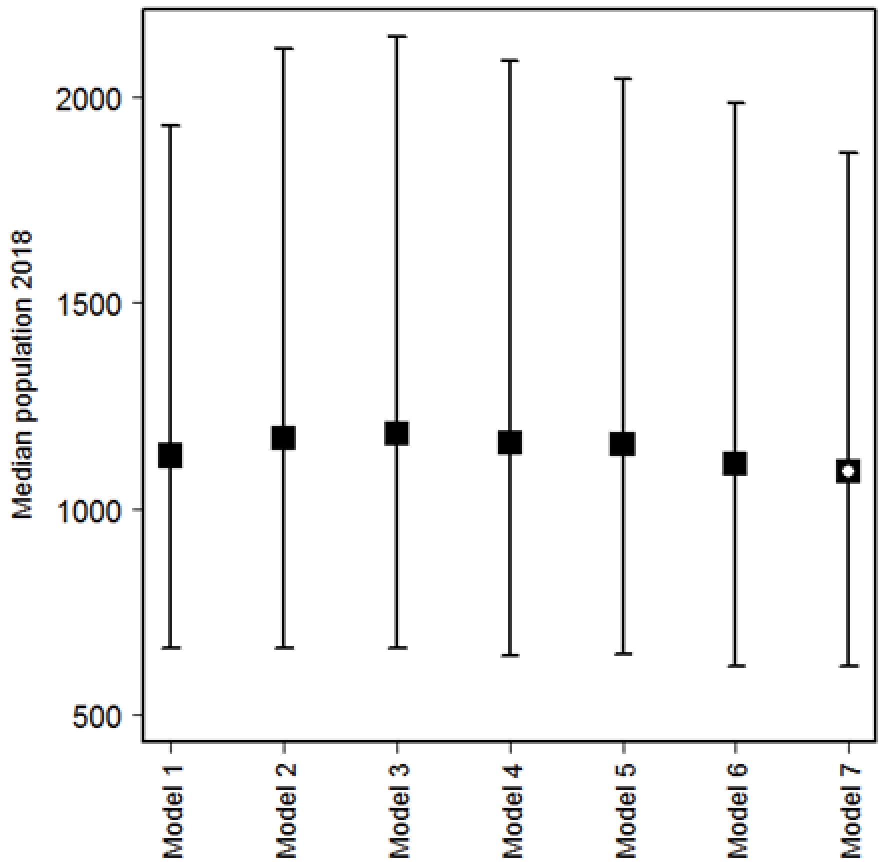

Figure 6. Sensitivity of median population estimates (squares) and 95% CI (Bars) to the hyper-parameters used in prior distributions (see Table 7). The white circle indicates the final model that was selected.

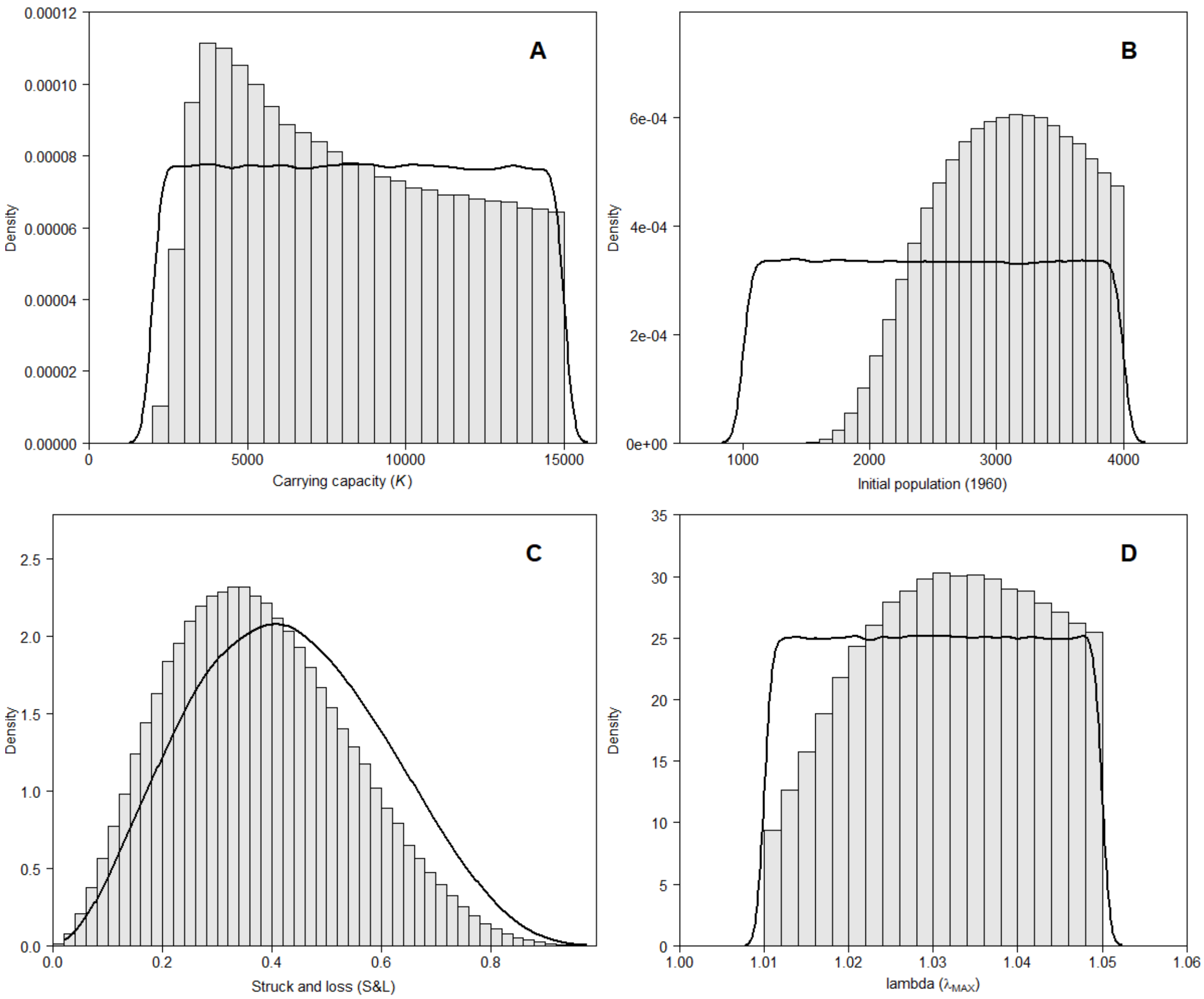

Figure 7. Plots show priors (lines) and posterior (histograms) for (A) carrying capacity (K), (B) initial population, (C) struck and loss (S&L), and (D) lambda (λ_{MAX}) when theta = 1.

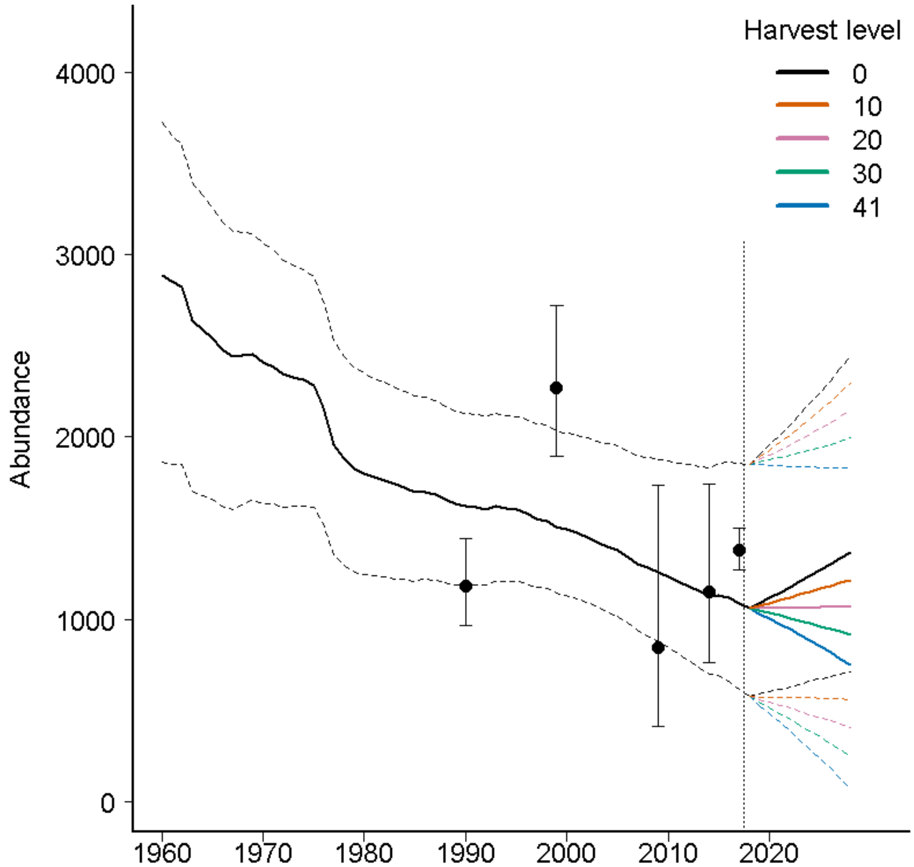

Figure 8. Estimated changes in abundance of CS beluga determined after fitting the population model to abundance estimates from aerial surveys flown between 1990–2017. The solid line indicates the median estimate and dotted lines represent the 95% Credibility Intervals. Beyond 2018 indicates future population projections at harvests of 0–41 beluga whales annually.

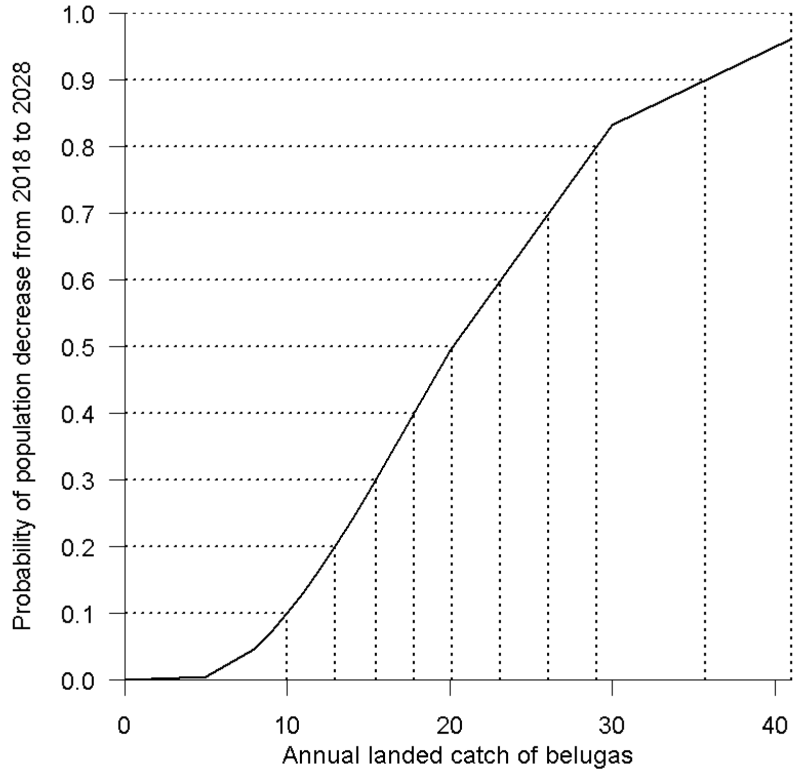

Figure 9. Probability of the Cumberland Sound beluga stock decreasing from the 2018 abundance estimate after 10 years of harvest, estimated by a stochastic Bayesian stock-production model (θ = 1) as a function of the landed catch of belugas every year. Dotted lines indicate levels of harvest (x-axis) corresponding to the probability of decline (y-axis).